

The experimental results demonstrate that, for different values of gas pressure and different size cylindrical containers, the entire histories of the electron and ion densities are the same if diffusion is the only loss process and if densities and time are scaled as $Ne^2\Lambda^2/\epsilon_0 KT$ and tD_*/Λ^2 , respectively. The charged-particle densities in helium decay at the same rate (ambipolar diffusion) if the characteristic diffusion length of the plasma container Λ is more than 86 times the spatially averaged Debye length $\langle\lambda_D\rangle = (\epsilon_0 KT/e^2\langle N_e\rangle)^{1/2}$. Also, in helium the ion current falls by a factor $(1.2 \pm 0.5) \times 10^5$ during the transition regime, after which the ions diffuse at their free rate. The factor that the ion current decreases during the transition should not be af-

ected by metastable atoms.

The numerical calculations by Kregel³ very closely predict the behavior of the electrons from the ambipolar regime to a density well into the transition regime. Discrepancy between the experimental results and Kregel's calculation at the lowest-measured values of electron density may be due to ionizing collisions between pairs of metastable atoms. This discrepancy is also observed when the experimental results are qualitatively compared with the numerical calculation presented in Ref. 4. While metastables may be the cause for the difference between experiment and the calculations, we cannot discount the possibility that the theory is incorrect.

*Work supported by the U. S. Atomic Energy Commission.

¹W. P. Allis and D. J. Rose, *Phys. Rev.* **93**, 84 (1954).

²I. M. Cohen and M. D. Kruskal, *Phys. Fluids* **8**, 920 (1965).

³Mark D. Kregel, *J. Appl. Phys.* **41**, 1978 (1970).

⁴M. A. Gusinow and R. A. Gerber, *Phys. Rev.* **5**, 1802 (1972).

⁵R. J. Freiberg and L. A. Weaver, *Phys. Rev.* **170**, 336 (1968).

⁶L. A. Weaver and R. J. Freiberg, *J. Appl. Phys.* **39**, 4283 (1968).

⁷R. A. Gerber, M. A. Gusinow, and J. B. Gerardo, *Phys. Rev. A* **3**, 1703 (1971).

⁸H. J. Oskam and A. R. DeMonchy (private communication).

⁹R. A. Gerber and M. A. Gusinow, *Phys. Rev. A* **4**, 2027 (1971).

¹⁰Mandred A. Biondi, *Rev. Sci. Instrum.* **22**, 500 (1951).

¹¹J. C. Slater, *Rev. Mod. Phys.* **18**, 441 (1946).

¹²G. E. Veatch and H. J. Oskam *Phys. Rev.* **184**, 202 (1969).

¹³M. A. Gusinow, A. Gerber, and J. B. Gerardo, *Phys. Rev. Lett.* **25**, 1248 (1970).

¹⁴H. J. Oskam and V. R. Mittlestadt, *Phys. Rev.* **132**, 1435 (1963).

¹⁵P. Patterson and E. C. Beaty, *Bull. Am. Phys. Soc.* **7**, 636 (1962).

¹⁶A. V. Phelps, *Phys. Rev.* **99**, 1307 (1955).

¹⁷M. A. Gusinow and R. A. Gerber, *Phys. Rev.* **2**, 1973 (1970).

¹⁸A. Wayne Johnson and J. B. Gerardo, *Phys. Rev. A* **5**, 1410 (1972).

Verification of the Lifshitz Theory of the van der Waals Potential Using Liquid-Helium Films

E. S. Sabisky and C. H. Anderson
RCA Laboratories, Princeton, New Jersey 08540

(Received 22 June 1972)

Accurate measurements are presented of the thickness of helium films on cleaved surfaces of alkaline-earth fluoride crystals at 1.38°K. The films were measured between 10 and 250 Å using an acoustic interferometry technique. The data are in excellent agreement with calculations based on the Lifshitz theory of van der Waals forces. Calculations of the film thickness on a variety of other substrates are also given.

I. INTRODUCTION

In 1881 van der Waals¹ introduced weak attractive forces between molecules to help explain the deviation in the properties of real gases from the ideal-gas law. The nature of these forces was shown by London² to be due to a neutral molecule possessing a fluctuating electric dipole moment which attracts neighboring molecules through the induced moment in these molecules. Casimir and Polder³ pointed out that the polarization of the neighboring molecules does not instantaneously follow the first molecule because the velocity of

light is finite. This force between molecules varies inversely as the seventh power of the distance between their centers for molecules which are close and inversely as the eighth power when the distance between molecules is large enough for retardation to be important.

The major difficulty of applying these theories to condensed systems or bodies is that the van der Waals force is not additive, and attempts to treat the problem from a perturbation point of view are not satisfactory. Lifshitz⁴ has developed a more comprehensive theory of this force which treats matter as a continuum with a well-defined fre-

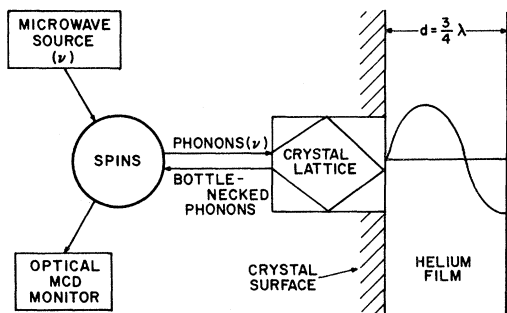


FIG. 1. Schematic representation of the method used to measure the properties of helium films adsorbed on alkaline-earth fluoride crystals.

quency-dependent dielectric susceptibility. A detailed and rigorous description of the molecular forces between solid bodies and a thin film on the surface of a solid body is given by Dzyaloshinskii, Lifshitz, and Pitaevskii⁵ (DLP). The paper by DLP shows that the formulas of London, and Casimir and Polder are contained as limiting forms of the Lifshitz formula. Most important, however, is that the general equations used to calculate the dispersion force require only information about the dielectric properties of the bodies. In principle, this information can be obtained from independent spectroscopic measurements. Parsegian and Ninham⁶ have applied this theory to a detailed study of dispersion forces between biological membranes. They have also shown that this theory only requires a partial knowledge of the frequency-dependent dielectric susceptibility of the bodies to give accurate results.

The first direct measurements of the van der Waals force between two solid bodies were made by Derjaguin and Abrikosova⁷ using two flat plates, both made of quartz (also using one made of quartz and the other of metal), at separations of 1000–4000 Å. These very difficult experiments have been continued by several groups,⁸ producing results which are in reasonable agreement with the retarded limit of the Lifshitz theory. These direct types of measurements have also been made⁹ in the regime where the forces are not retarded, and the results demonstrated the transition from non-retarded to retarded behavior.

Schiff¹⁰ in 1941 noted that the relatively thick liquid-helium films observed on the walls of containers are formed by the van der Waals force. Although there has been some controversy as to the importance of additional forces, DLP have examined this problem in detail and have given an explicit expression relating the van der Waals force to the film thickness. For some unknown reason, there appear to be only minor attempts to interpret past measurements of the helium film

thickness in terms of the explicit expression of DLP. We have made extensive measurements of the helium film thickness on atomically flat regions of freshly cleaved surfaces of alkaline-earth fluoride crystals. Richmond and Ninham¹¹ have shown that our preliminary results¹² are in good agreement with the Lifshitz theory. This paper presents a detailed description of our experiments and a comparison of our extensive measurements with calculations based on the Lifshitz theory. The remarkable agreement that is found between theory and experiment provides a strong confirmation of this theory. Also, the results provide an accurate scale for the thickness of liquid-helium films on these surfaces.

II. EXPERIMENTAL

A. Method

The helium film thickness in these experiments is measured through the detection of simple acoustic standing-wave patterns of a given frequency set up between the substrate, which supports the film, and the helium liquid-gas interface. The film thickness is determined by simply counting the number of wavelengths contained across the film and calculating the magnitude of the wavelengths from the exciting frequency. The substrates in these experiments are single crystals of CaF_2 , SrF_2 , and BaF_2 doped with 0.02 mol% of the paramagnetic ion divalent thulium. These doped crystals have been studied in detail to demonstrate a new acoustic-phonon spectrometer concept.¹³

The interaction between the paramagnetic spins and the helium film is best understood as follows, with reference to Fig. 1: The paramagnetic spins are tuned by an external magnetic field into resonance with monochromatic microwave radiation. The microwave power absorbed by the spins is re-radiated into the crystal lattice as incoherent monochromatic acoustic phonons of the same frequency, which at the low temperatures used in the experiments travel unimpeded until they hit the surface of the crystal. The crystal is mounted inside a can containing helium gas which coats the crystal with a liquid-helium film. However, the acoustic mismatch between the crystal and liquid helium is quite large, so very few phonons are lost through a collision at the surface. This results in an excess of phonons at the resonant frequency being formed inside the crystal, the density of which depends directly on the phonon loss rate into the helium film. These extra phonons can be detected through their slight warming effect on the thulium spins. We have preferred to detect the temperature of the spin system using the magnetic circular dichroism of the optical-

absorption bands of thulium because it is a very sensitive method which is independent of the exciting microwave frequency.¹⁴ If the film thickness is changed through the addition or removal of helium or if the microwave frequency is adjusted so that the film thickness is equal to an odd multiple of a quarter-wavelength, the coupling of the resonant acoustic radiation into the helium film is enhanced. The nature of the damping of these resonant modes, and therefore where the acoustic power goes, is not understood, although eventually the energy is lost into the surrounding helium gas. This enhanced coupling of the phonons out of the crystal reduces the excess number of phonons in the warm resonant mode, and the spins are observed to become slightly cooler.

To a very good approximation the resonances can be considered as compressional standing waves, with a node at the hard crystal surface and an antinode at the free liquid-gas interface. Thus the lowest-order mode occurs when the film thickness is one-quarter of a wavelength, and higher modes occur for odd multiples of a quarter-wavelength. The phonons in the crystal couple only with these simple standing-wave modes in the film because the velocity of sound in the crystal is an order of magnitude larger than it is in liquid helium. In effect, even acoustic waves traveling almost parallel to the crystal surface are refracted upon going into the liquid helium to within a few degrees of the normal direction. Therefore, when the spin temperature is observed to go through a minimum the film thickness is given to first order by

$$d_A = N\lambda = \frac{NC_0}{\nu}, \quad N = \frac{1}{4}, \frac{3}{4}, \frac{5}{4} \dots, \quad (1)$$

where d_A is what we call the simple acoustic thickness, N is the number of wavelengths in the resonant mode, and λ is the acoustic wavelength calculated from the velocity of sound in bulk liquid helium, C_0 , and the microwave frequency ν . The small corrections to this expression which are necessary to obtain the "true" film thickness are discussed later.

The resonances were first observed in an experiment designed to measure the change in phonon lifetimes when a crystal is removed from liquid helium and placed in very-low-density helium gas. In these experiments the phonons were generated by irradiating the spins with microwave power at one end of the crystal and detected by the spins at the other end, which was shielded from the microwave power. In these polished crystals, a strong quarter-wave resonance along with a weak three-quarters-wave resonance would generally be observed. In addition, a very broad weak peak at lower gas pressures, where the film

is only two statistical atomic layers thick, is observed. The origin of the broad peak is not known and has not been extensively studied.

In order to achieve isolation from the exciting microwave power in these first experiments, the crystal had to be cut to a definite shape and therefore the surfaces had to be polished. These highly polished surfaces are extremely rough on an atomic scale and this limits the number of resonances that can be observed. In order to observe a large number of resonances, crystals with cleaved surfaces had to be used, which Strehlow and Cook¹⁵ have shown have an appreciable fraction of their surface that apparently is atomically flat. The need for atomically flat surfaces is readily understood since at the highest frequency used in these experiments, 58 GHz, the acoustic wavelength in liquid helium is only 40 Å. It must also be understood that the whole surface need not be atomically flat. That the surface has to be atomically flat in order for the resonances to be sharp means that regions which are disturbed by dirt, cleavage steps, and other imperfections will not contribute to the resonances and thus do not affect the results. This experiment automatically selects the atomically flat clean parts of the surface!

In order to be able to work with oddly shaped freshly cleaved crystals (the cleavage planes have a [111] orientation in these crystals), we choose to use the same spins to generate and detect the phonons. This is achieved by only moderately heating the spins with the microwave radiation so that the effect of the warm phonons on the spin system can also be observed. The optimum condition for maximum sensitivity is attained when the microwave power is set to heat the spins 30% hotter than the bath. The original geometry of the first experiments allows absolute phonon decay rates to be measured; while this second geometry lacks this feature, it still allows the position of the resonant peaks to be observed as minima in the spin temperature.

B. Apparatus

The first results¹² published on the film thickness measured as a function of the chemical potential were made in an apparatus using a large glass can to seal the end of the waveguide from the liquid-helium bath. This was changed to the design shown in Fig. 2 because it was thought the original measurements might have been affected by thermal gradients, which turned out not to be the case. The basic crystal holder, made from pure copper, has two optical windows for the monitor light to pass through, which are sealed on with indium *O* rings. The unit as a whole can quickly be sealed, also with indium, onto the end of a length of *K*-band waveguide (i. d. = 0.43 × 1.07 cm).

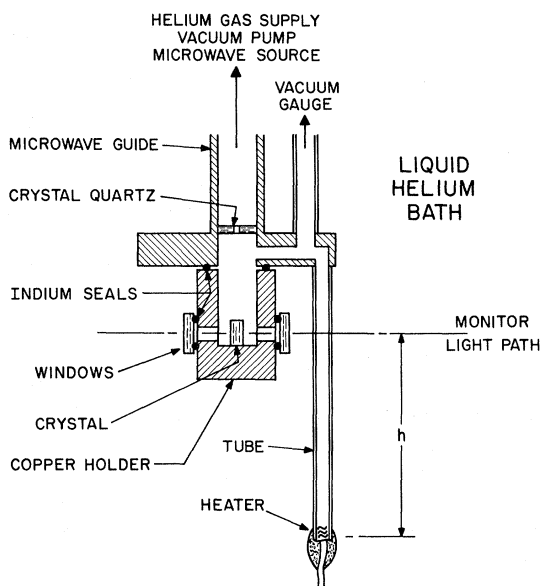


FIG. 2. Schematic drawing of the cross section of the vacuum can.

A piece of crystal quartz with a small hole in it is glued in place slightly up the waveguide to prevent thermal radiation from the room-temperature end of the waveguide from entering the section holding the crystal. To one side and rotated 90° with respect to the optical windows is a $\frac{1}{8}$ -in. i. d. stainless-steel tube which is connected to a high-precision differential capacitive pressure gauge. Below this is a length of copper tubing extending a length h below the level of the crystal and closed at the bottom, sometimes with an electrical heater epoxyed in place. The upper end of the waveguide can be quickly connected to a vacuum system and a helium-gas handling system, as well as to a variety of microwave sources.

This apparatus is inserted into an ordinary glass helium-Dewar system with an unsilvered area to allow the monitor light to pass through both the helium and liquid-nitrogen Dewars. The helium-bath temperature is stabilized with an electronic controller using an electrical heater. The optical system, including the method for detecting magnetic circular dichroism, has been described extensively elsewhere.¹³ The magnetic field for tuning the spins is supplied by a 12-in. magnet stabilized with a Hall probe. The magnetic field of the magnet was calibrated using a nuclear-magnetic-resonance (NMR) probe. In some cases, the magnetic field reading when the spins were tuned into resonance with the applied microwave radiation was used to calculate the frequency of the microwave source, using the paramagnetic-resonance parameters previously measured. The precision of the frequency obtained in this way is slightly

better than one part in 10^3 . The microwave frequency was repeatedly swept over 100 MHz, which is more than the electron-paramagnetic-resonance (EPR) linewidth, to ensure that the entire resonance line was uniformly heated. This gives the phonons generated a bandwidth of about 60–80 MHz which is the range of the thulium linewidths in these crystals. Only one of the two major thulium hyperfine lines was used in these experiments, usually the low-magnetic-field line.

An important feature in the new measurements reported here is the use of a commercial capacitive-type differential pressure gauge with a sensitivity of 10^{-5} Torr, which replaced the Pirani gauges used in the first measurements. One side of this gauge was connected to the $\frac{1}{8}$ -in.-diam stainless-steel tube leading to the crystal holder and the other side was connected to a similar tube which extended down into the liquid-helium bath. It was impossible because of space limitations to terminate the reference side in a system identical to that which held the crystal. Therefore, the gas pressure in the two sides of the capacitive gauge was not identical when the pressure in the can was at saturated vapor pressure. The differential gauge typically had a reading of 10^{-4} Torr instead of zero in this case. Whatever the cause of this small pressure difference, it is not expected to appreciably change when the pressure in the can is reduced over the range of pressures used in these experiments. The gas pressures in the can were obtained from the differential pressure readings with respect to the reading at the saturated vapor pressure which is taken as the zero. This differential pressure is defined as ΔP where $\Delta P = P_0 - P$ and P_0 is the saturated vapor pressure.

C. Procedure

The crystals of CaF_2 , SrF_2 , and BaF_2 doped with 0.02 mol% thulium were obtained from Optovac, and the thulium was reduced to the divalent state by us. Chips with no dimension larger than 2 mm were cleaved from the boules in air, immediately set in the crystal holder, and held in place with a piece of styrofoam pushed down on top of it. The holder was then sealed onto the end of the waveguide and the interior pumped down to a pressure below 10^{-4} Torr before being immersed in the liquid-helium bath. This entire procedure could be carried out in 15 min.

Helium gas was introduced into the apparatus until the pressure saturated, indicating that a small amount of bulk liquid had condensed at the bottom of the copper tube. Using the circular dichroism monitor of the spin temperature it was possible to tune the spins into resonance with the applied microwave radiation and adjust the power level so that the spin temperature was about 30%

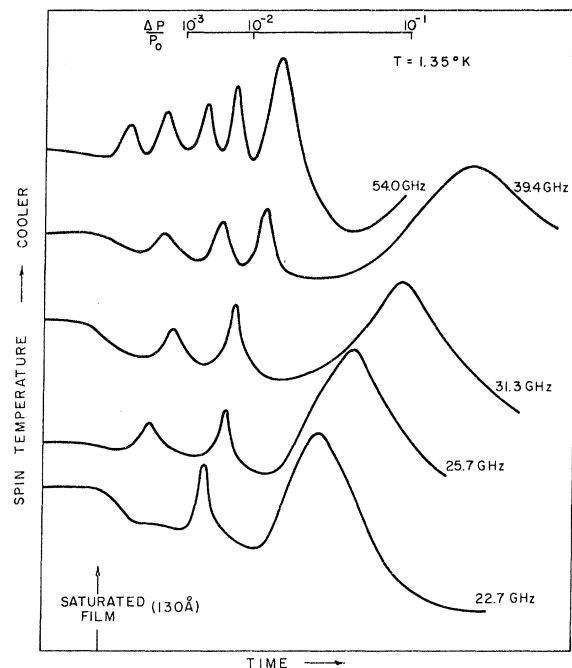


FIG. 3. Acoustic wave interference in thin films of liquid helium adsorbed on cleaved surfaces of SrF_2 detected through its effect on the spin temperature of divalent thulium in the crystal. The spin-temperature scale is in arbitrary units with the maximum excursion of each curve of $30 \text{ m}^\circ\text{K}$. For convenience of display, the horizontal scale is uniform in time.

hotter than the bath temperature. The circular dichroism signal was then greatly amplified and put onto the y axis of an x - y recorder. The x axis was driven by the output of the differential pressure gauge. The helium gas in the apparatus was then very slowly pumped out, taking as long as 30–60 min for a typical run. At saturation the helium coats everything inside the apparatus with a liquid film, the thickness of which on the crystal is determined by the height h of the crystal above the lowest point in the interior of the system where the bulk liquid has collected. When the helium gas is slowly pumped away nothing happens until the bulk liquid is removed and then the film thins, initially fairly uniformly as a function of time. Each time the film goes through one of the resonances the spin temperature cools and the circular dichroism signal increases. A figure from our original article¹² showing a series of such runs at several different frequencies is reproduced in Fig. 3. From these records it is possible to associate the top of each peak quite accurately with a differential pressure reading ΔP . It is also possible to obtain the total number of peaks observed up to saturation.

The following features were noted about the measurements: (i) The new results, for both

saturated and unsaturated films, are in excellent agreement with the less precise original results. (ii) The peak positions were not sensitive to the microwave and optical power, except that excessive power can burn off thin films. Typically the power level was of the order of tens of nanowatts. (iii) The pressure differential readings for peaks very close to saturation were found to be slightly dependent on the rate at which the helium gas was removed, and for careful readings in this regime the pump rate was kept very low. The experimental design did not allow us to take accurate data as helium gas was added to the can. (iv) The saturated film thickness was found to be independent of temperature between 1.35 and 1.8°K , the limit of this measurement. The signal-to-noise ratio progressively decreases as the temperature increases, making it difficult to accurately identify the saturation point at higher temperatures. (v) Some preliminary measurements of the resonances were made as a function of temperature up to 2.1°K ; small changes were observed in the apparent thickness actually indicating temperature dependence on the velocity of sound. The onset point where the film turned normal could usually be noted as a small sharp increase in the spin temperature and the resonances could be observed in this normal film. The velocity of sound apparently decreases abruptly by a small amount as the film passes through the onset transition. (vi) The same results were found on a sample cleaved in the system after being cooled to helium temperatures as were found on the samples cleaved in air. Since the apparatus for doing this was difficult to use this was done only once. (vii) In one experiment small chips of CaF_2 and BaF_2 were mounted next to one another and measurements made alternatively on each, the monitoring light being used to select each sample separately. Surprisingly, the film thicknesses on both substrates were identical to the precision of the experiment. The calculations discussed in Sec. III show that all three materials, CaF_2 , SrF_2 , and BaF_2 , should have the same film thickness. All the final results tabulated in this paper were taken on SrF_2 at 1.38°K except for a couple of saturated film points.

D. Data Reduction

Discussed in this section are the details of how the film thickness is obtained from the order of each resonance peak and how the chemical potential of the gas in the vicinity of the crystal is obtained from the pressure differential ΔP associated with each peak. In this way the potential due to the van der Waals force of the helium in the film surface is found for thicknesses in the range 10 – 250 \AA .

In our first paper¹² the film thickness was calculated from the order of a resonance peak N using the simple acoustic length given by Eq. (1). The value of the phase velocity used for the GHz frequencies of these experiments was that measured at MHz frequencies in bulk liquid at 1.38°K, namely, 236.6 m/sec. Since then we have found that two small corrections have to be added to this simple formula: the dispersion of the velocity of sound in the bulk liquid and a frequency-dependent phase-shift correction introduced at the boundaries. These corrections can best be visualized by assuming that the helium has uniform properties across the film identical to bulk liquid except for the boundary region extending a somewhat arbitrary distance from the substrate. In this region the helium is compressed by the van der Waals force, and so the velocity of sound rapidly changes as a function of distance. Since this region is small compared to the wavelengths used in these experiments it is possible to use a standard boundary-layer technique of replacing the real wave with a wave of constant phase velocity which originates at a node a distance $d_0(\nu)$ from the substrate; $d_0(\nu)$ is defined as the phase shift. In effect the real wave experiences a phase shift relative to an ideal wave, for which the phase velocity undergoes an infinitely sharp change between the solid substrate and the liquid helium. It is reasonable to expect the perturbations at the substrate-liquid interface to be much larger than any effect at the liquid-gas interface because the wave is an antinode at this second boundary. However, the phase shift measured is the net resultant of both and we cannot experimentally separate the two. If the measured phase shift is due entirely to the substrate-liquid boundary region it is possible to obtain a complete description of the dynamics of this interesting region from the frequency dependence of the phase shift, which should provide fundamental insight into the Kapitza resistance. In this experiment it is most convenient to measure the phase shift in units of length.

The "true" film thickness is therefore given by the modified expression

$$d = \frac{C_0 N [1 + \delta(\nu)]}{\nu} + d_0(\nu), \quad (2)$$

where $\delta(\nu)$ is the dispersion correction and $d_0(\nu)$ is the phase-shift correction. It is possible to measure the *relative* dispersion and phase shift at different frequencies by making precise frequency measurements of two or more modes at a given film thickness. This is best demonstrated by considering the difference between the simple acoustic thickness calculated for two different modes measured in the same film, which from Eqs. (1) and (2) is given by

$$\Delta d = C_0 \left(\frac{N_2}{\nu_2} - \frac{N_1}{\nu_1} \right) = C_0 \left[\delta(\nu_1) \left(\frac{N_1}{\nu_1} \right) - \delta(\nu_2) \left(\frac{N_2}{\nu_2} \right) \right] + d_0(\nu_1) - d_0(\nu_2). \quad (3)$$

The factors (N_2/ν_2) and (N_1/ν_1) are observed experimentally to be the same to within a few percent and negligible error is introduced by rewriting this expression as

$$\Delta d = d_A [\delta(\nu_1) - \delta(\nu_2)] + d_0(\nu_1) - d_0(\nu_2), \quad (4)$$

where d_A is the acoustic thickness calculated for either frequency or taken as the mean of the two. This equation shows that the relative dispersion and relative phase shifts can be separated by making measurements of Δd at more than one film thickness, the dispersion part increasing with film thickness and the phase-shift part remaining fixed.

The results of a series of experiments to determine Δd for a variety of film thicknesses and frequencies in order to obtain the relative dispersion and phase shifts have recently been published.¹⁶ If the data given in Ref. 16 are inspected carefully it is seen that there are in reality only two data points on the dispersion, 20–37 and 35–55 GHz. Therefore many two-parameter models of the dispersion will fit the data. It is significant, however, that the data can be essentially represented by a simple straight line. For the purposes of this paper, all that is important is the value of the dispersion and not the model. The value for the relative dispersion is given by

$$\delta(\nu) = (6.3 \pm 0.7) \times 10^{-13} \nu + (0 \pm 8) \times 10^{-25} \nu^2, \quad (5)$$

with ν given in units of hertz. The relative phase shift is numerically fitted best by the formula

$$d_0(\nu_1) - d_0(\nu_2) = (-0.12 \pm 0.01) \times 10^{-9} (\nu_1 - \nu_2) + (6 \pm 1) \times 10^{-22} (\nu_1^2 - \nu_2^2). \quad (6)$$

It is possible to define an absolute scale for the phase shift by requiring the thickness scale obtained by the acoustic measurements to go to zero when the length scale associated with the van der Waals force goes to zero. For example, the van der Waals potential is expected to have a simple inverse-cubic dependence on film thickness at short distances, and therefore the scale length is approximately proportional to the measured potential to the minus one-third power. Figure 4 shows that $\nu^{-1/3}$ near the origin is linearly proportional to the acoustic thickness with all its corrections except the frequency independent part of the phase shift d_0 . By taking the intercept where $\nu^{-1/3}$ goes to zero as a measure of d_0 we ensure that the acoustic and van der Waals thickness scales both refer to the same origin. The value of d_0 from the intercept is 5.8 Å. A recent measurement¹⁷ at 135 GHz of -1.8 Å is reasonably

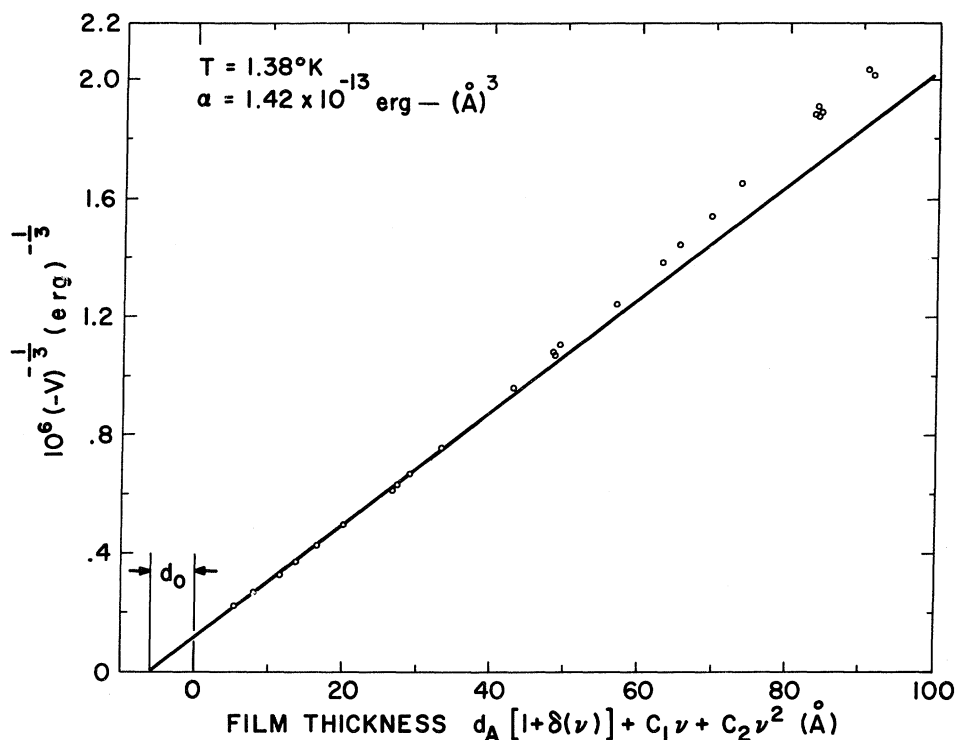


FIG. 4. Minus one-third power of the van der Waals potential as a function of the helium film thickness on a SrF_2 substrate. The film thickness does not include the frequency-independent part of the phase shift d_0 . The form of the phase shift is assumed as $d_0(\nu) = d_0 + c_1\nu + c_2\nu^2$.

consistent with our values. Although this curve cannot be extrapolated to zero frequency with confidence, 5.8 \AA not really having any physical significance, the phase shift at very low frequencies is much larger than we have earlier estimated.

The chemical potential V_c per helium atom of the gas in the vicinity of the crystal is given by

$$V_c = kT \ln[P_0(T)/P_x], \quad (7)$$

where kT is the Boltzmann constant times the temperature, $P_0(T)$ the vapor pressure of liquid helium at the temperature T , and P_x the gas pressure at the crystal. The van der Waals potential per helium atom in the liquid helium surface $V(d)$ is the negative of V_c , $V(d) = -V_c$. If P_B is the pressure at the lowest point in the interior of the system, Eq. (7) can be rewritten

$$V_c = mgh + kT \ln[P_0(T)/P_B], \quad (8)$$

where mgh is the gravitational potential for an atom at a height h above the bottom. We now assert that the pressures relative to the saturated condition as measured at the gauge are proportional to the pressure at the bottom of the interior of the system relative to the saturated vapor pressure of the bulk liquid which collects there. Thus we obtain

$$\frac{P_0(T) - P_B}{P_0(T)} = \frac{\Delta P}{P_0},$$

where ΔP and P_0 are the measured quantities previously discussed. The chemical potential is therefore calculated using the equation

$$V_c = mgh + kT \ln[P_0/(P_0 - \Delta P)]. \quad (9)$$

The natural units we find using this approach for the potential are ergs per helium atom. Traditionally the potential for saturated films is measured in units of height, $1 \text{ cm} = 6.55 \times 10^{-21} \text{ erg}$, for the obvious reason that it gives the helium thickness profile as a function of height. For thin unsaturated films it has been usual to define the potential in units of degrees kelvin and the film thickness in units of layers of liquid helium (1 layer = 3.60 \AA). The constant of proportionality α of the van der Waals potential when it is approximated by a simple inverse-cube law then has the units of degrees kelvin (layers)³.

The experimental data taken on SrF_2 at 1.38°K for both saturated and unsaturated films are given in Table I and are plotted in Fig. 5. The closed points in Fig. 5 are for unsaturated films, while the open circles are for saturated films. Each datum point represents the average of two or more measurements. Typical reproducibility of the po-

tential is about $\pm 2\%$ over the entire range. The major uncertainty of about 1% in the film thickness comes from the value of C_0 used in Eq. (2). The

phase-shift correction is known from experiment to about ± 0.5 Å. The major uncertainty in the dispersion correction, which at most is a 3% cor-

TABLE I. Experimental data of van der Waals potential and helium film thickness at 1.38 °K.

Frequency (GHz)	Wave number (N)	$-V(d)$ ($\text{erg} \times 10^{20}$)	$d_A = NC_0/\nu$ (Å)	$d_A[1 + \delta(\nu)]$ (Å)	$d = d_0(\nu) + d_A[1 + \delta(\nu)]$ (Å)
Unsaturated films					
57.74	0.25	8680	10.24	10.61	11.5
57.65	0.25	8500	10.26	10.63	11.5
48.58	0.25	5130	12.18	12.55	14.0
39.13	0.25	2745	15.12	15.49	17.6
35.13	0.25	1900	16.84	17.21	19.5
34.6	0.25	1875	17.10	17.47	19.8
30.45	0.25	1270	19.43	19.80	22.5
26.70	0.25	853	22.15	22.52	25.4
20.80	0.25	423	28.44	28.81	32.3
57.74	0.75	397	30.73	31.83	32.7
57.65	0.75	389	30.78	31.89	32.8
19.16	0.25	332	30.87	31.24	34.8
48.58	0.75	226	36.53	37.65	39.1
39.13	0.75	112	45.35	46.47	48.6
35.13	0.75	77.0	50.51	51.63	53.9
57.74	1.25	81.0	51.22	53.05	54.0
57.65	1.25	80.8	51.3	53.15	54.1
34.60	0.75	75.5	51.29	52.4	54.7
30.45	0.75	51.7	58.28	59.4	62.1
48.58	1.25	46.6	60.88	62.75	64.2
26.70	0.75	33.0	66.46	67.56	70.5
57.74	1.75	27.7	71.71	74.27	75.2
57.65	1.75	27.2	71.82	74.41	75.3
39.13	1.25	22.0	75.58	77.45	79.6
35.13	1.25	15.2	84.19	86.05	88.4
48.58	1.75	15.0	85.23	87.85	89.3
34.60	1.25	14.0	85.48	87.35	89.7
20.80	0.75	14.9	85.31	86.43	89.9
57.74	2.25	12.3	92.2	95.49	96.4
57.65	2.25	11.8	92.34	95.67	96.6
19.16	0.75	11.8	92.61	93.72	97.3
30.45	1.25	9.6	97.13	99.0	101.7
39.13	1.75	6.7	105.81	108.43	110.5
48.58	2.25	6.3	109.58	112.95	114.4
26.70	1.25	6.0	110.77	112.6	115.5
57.74	2.75	5.7	112.69	116.71	117.6
57.65	2.75	5.5	112.86	116.93	117.8
35.13	1.75	4.7	117.86	120.47	122.8
57.74	3.25	3.15	133.17	137.93	138.8
Saturated films					
		6.55	109	112.4	113.7
		4.19	121	123.6	126.0
		4.13	123	125.6	128.0
		3.73	125	129.1	130.5
		2.62	140	144.7	145.7
		1.96	154	159.6	160.6
		1.90	155	158.4	160.7
		1.31	171	176.9	177.9
		0.82	193	198	200
		0.59	215	220	222
		0.36	240	245	247

rection, is in its absolute value. A reasonable estimate of this error is one-half of the dispersion at 20 GHz, the lowest frequency used in the dispersion measurements obtained, assuming the linear behavior continues to the origin. This gives an uncertainty of 0.5% in the film thickness.

III. CALCULATION OF VAN DER WAALS FORCE

Richmond and Ninham¹¹ have calculated the van der Waals potential for helium films on the alkali-earth fluoride substrates using the computer program developed by Parsegian and Ninham¹⁸ for the full Lifshitz formula.⁵ They obtained good agreement with our earlier data. Presented here is a refined calculation using more comprehensive

models for the dielectric susceptibility functions. The results are compared to the more precise data given in Sec. II. The calculated film thickness for a given potential is shown to be fairly insensitive to the model parameters and in excellent agreement with the data. Similar calculations for a selected number of substrates are also presented. Finally, the accuracy of more tractable approximations to the full Lifshitz formula is explored.

A. Lifshitz Formula and Dielectric Models

The exact Lifshitz formula for the van der Waals potential per unit volume of helium in the film surface is given by

$$V(d) = \frac{\hbar}{2\pi^2 C^3} \int_0^\infty \int_1^\infty p^2 \zeta^3 \epsilon_3^{3/2} \left\{ \left[\frac{(S_1+p)(S_2+p)}{(S_1-p)(S_2-p)} \exp\left(\frac{2p\zeta d}{C\sqrt{\epsilon_3}}\right) - 1 \right]^{-1} + \left[\frac{(S_1+p\epsilon_1/\epsilon_3)(S_2+p\epsilon_2/\epsilon_3)}{(S_1-p\epsilon_1/\epsilon_3)(S_2-p\epsilon_2/\epsilon_3)} \exp\left(\frac{2p\zeta d}{C\sqrt{\epsilon_3}}\right) - 1 \right]^{-1} \right\} dp d\zeta, \quad (10)$$

where $S_\alpha = (p^2 - 1 + \epsilon_\alpha/\epsilon_3)^{1/2}$, $\alpha = 1$ and 2 , $2\pi\hbar$ is Planck's constant, d is the film thickness, and C is the velocity of light in a vacuum. ϵ_1 , ϵ_2 , and ϵ_3 represent the dielectric susceptibilities, evaluated on the imaginary frequency axis at frequencies $\omega = i\zeta$, of (1) the substrate, (2) the helium vapor ($\epsilon_2 = 1$), and (3) liquid helium. These dielectric functions are positive real functions which decrease monotonically from the static dielectric constant ϵ_0 for $\zeta = 0$ to unity as ζ approaches infinity. Because of the weak dependence the integral has on the thickness d we have defined a positive function $\alpha(d)$ as

$$\alpha(d) = -d^3 V(d) \quad (11)$$

and made the detailed comparison to this function. If the potential in Eq. (10) is divided by the Boltzmann constant then $\alpha(d)$ has the usual units of degrees kelvin (layers)³. To compare Eq. (10) with the energy per helium atom which we use, the potential has to be multiplied by the volume a helium atom occupies in the liquid $(3.6 \text{ \AA})^3$.

Following Parsegian and Ninham¹⁸ we represent the dielectric functions as a sum of Lorentzian terms with the small corrections due to damping left out, i. e.,

$$\epsilon(i\zeta) = 1 + \sum_n \frac{A_n}{1 + (\zeta/\omega_n)^2}. \quad (12)$$

The ω_n are a set of resonant frequencies and the constants A_n multiplied by ω_n^2 represent a measure of the oscillator strength associated with each resonance. The dielectric function is written in this way because it is essential that the optical di-

electric constant be reproduced accurately, the results being less sensitive to the number and location of the resonant frequencies used. We do not follow Richmond and Ninham¹¹ in using the extremely-high-frequency limiting form for the dielectric function given by

$$\epsilon(i\zeta) \rightarrow 1 + \frac{4\pi N_e e^2}{m\zeta^2}, \quad (13)$$

where e , N_e , and m are the electronic charge, density, and mass, respectively. Instead, we have found it convenient to calculate the effective electronic number n_e per helium atom or primitive cell of the substrate for a particular set of model parameters to see if they are consistent with this limiting form. That is, we have

$$\sum_n A_n \omega_n^2 = \frac{4\pi n_e e^2}{mB}, \quad (14)$$

where B is the molecular volume; n_e , however, is not the total number of electrons which was used by Richmond and Ninham.¹¹

B. Dielectric Functions

The dielectric function for liquid helium can be represented by the three major transitions¹⁹ of atomic helium centered at the 1^1S-2^1P transition (21.2 eV), the 1^1S ionization limit (24.6 eV), and the double ionization transition (79 eV). By requiring the first two resonances to have relative oscillator strengths¹⁹ of 1-3 and the net oscillator strength of all three bands to give $n_e = 2$, the following function is obtained:

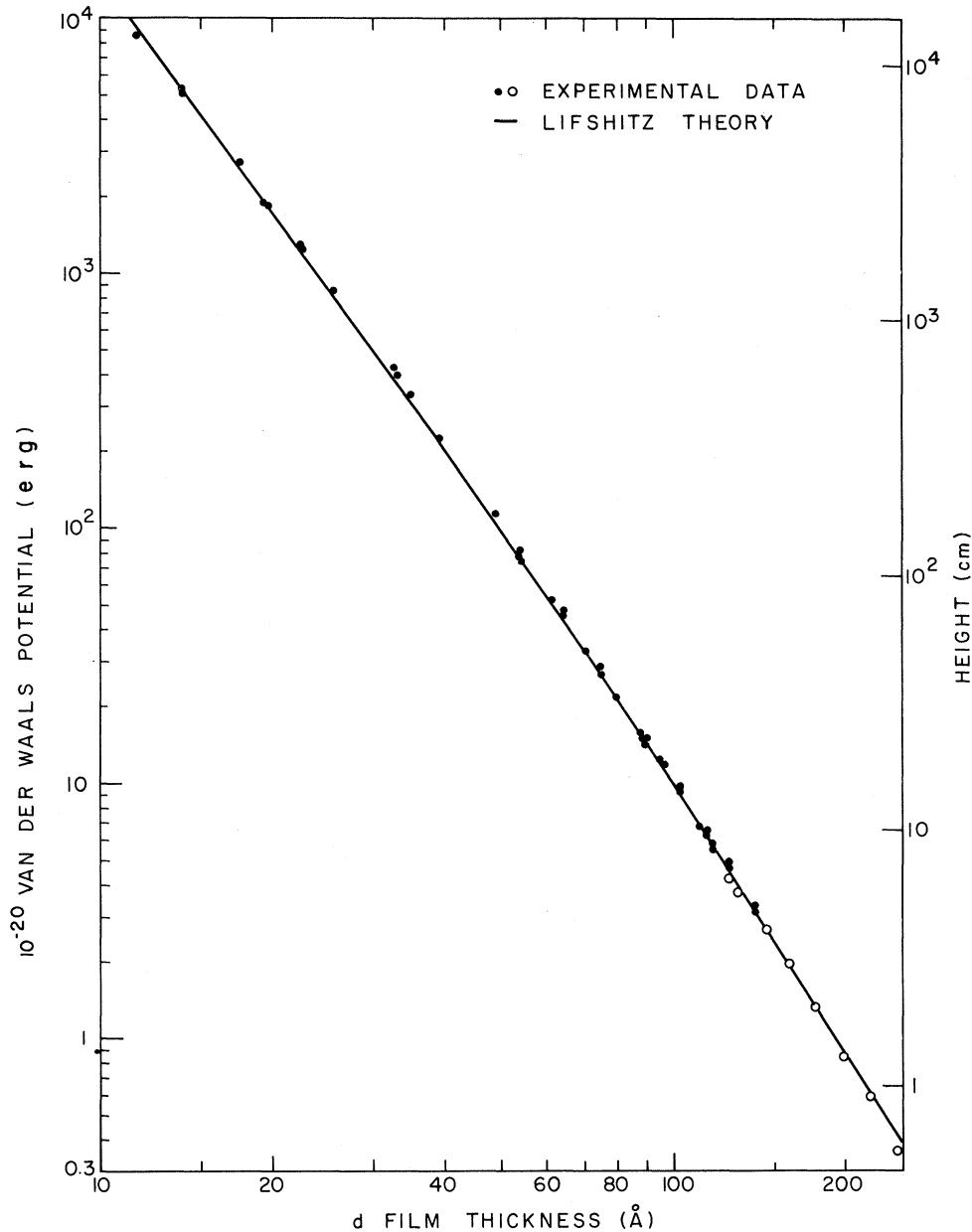


FIG. 5. van der Waals potential of a helium atom on the surface of the helium film which is adsorbed on a SrF_2 cleaved surface as a function of the film thickness at 1.38°K. The data represented by closed and open points are for unsaturated and saturated films, respectively. The solid line represents the theory of Lifshitz.

$$\epsilon_3(i\xi) = 1 + \frac{0.016}{1 + (\xi/\omega_1)^2} + \frac{0.036}{1 + (\xi/\omega_2)^2} + \frac{0.0047}{1 + (\xi/\omega_3)^2}, \quad (15)$$

where ω_1 , ω_2 , and ω_3 are 3.22×10^{16} , 3.74×10^{16} , and 12×10^{16} rad/sec, respectively. This function gives the correct dielectric constant of 1.057 and also produces the effective number of electrons per helium atom: two. For calculations other than for the SrF_2 substrate the third band was dropped and the constants of the first two terms

changed to 0.014 and 0.043, respectively, the difference in the calculated potential being about 3% at 10 Å and vanishingly small for thicker films.

This simple dielectric function for helium introduces an effective cutoff of the integral in Eq. (10) for frequencies above 4×10^{16} (25 eV) and therefore makes it unnecessary to obtain details about the substrate dielectric function for frequencies much above this. There is also a cutoff introduced by the exponential factor in the inte-

grand at the frequency $\xi = C/2d$ (1.5×10^{17} at $d = 10$ Å), which also reduces the need for detailed information about the substrate at extremely high frequencies. It is also this exponential cutoff which makes the calculation become more reliable at large values of d , since the dielectric response function at low frequencies is approximately equal to the optical dielectric constant.

Fortunately, the optical and dielectric properties of the alkaline-earth fluorides have been extensively studied at energies up to 50 eV. The available data were handled in the following manner: The properties of the infrared lattice bands were taken from the measurements of Bosomworth.²⁰ Constraints on the sums over the remaining electronic bands were obtained by plotting the tabulated square of the optical index of refraction n^2 as a function of ω^2 and making the correlation to the expression

$$n^2(\omega) - 1 \approx \sum \frac{A_n}{1 - (\omega/\omega_n)^2} \approx \sum A_n + \omega^2 \sum \frac{A_n}{\omega_n^2}. \quad (16)$$

Values for $\sum A_n$ and $\sum (A_n/\omega_n^2)$ can now be obtained from the intercept and slope of the curve, respectively. Data on the optical dielectric constant of SrF₂ are not available and values for the above constraints were obtained by interpolating between the values obtained for CaF₂ and BaF₂. The values for $\sum A_n$ were also checked against the values of ϵ_∞ given in Table I of Bosomworth.²¹ Recent²¹ ultraviolet-reflection data have been reported on all three materials. These data give good locations for the major electronic transitions up to 35 eV. We also used the results of older work²² which gave a plot of the cumulative effective electron number of CaF₂ as a guide for the oscillator strengths. A ten-band model of the uv spectrum of CaF₂ satisfying the constraints given above was first tried. It was found that this produced a function which was represented just as well by a simpler three-band model with frequencies centered at the three main groups of transitions observed in these materials. Similar three-band models

were then generated for SrF₂ and BaF₂, using the uv-reflection data as a guide for both band positions and intensities. The final resulting parameters, including the infrared band, are given in Table II. The effective number of electrons per primitive cell is approximately 12, which is the number of p electrons in two F⁻ ions. These model parameters have no physical meaning in themselves; they are merely used to provide a reasonable facsimile to the dielectric function. Later it will be shown how insensitive the net results are to these parameters.

C. Results of Calculation

The results of the calculation using the program of Parsegian and Ninham¹⁸ to evaluate the Lifshitz formula with the parameters in Table II for SrF₂ is represented by the solid line in Figs. 5 and 6. In order to better exhibit the deviations from the inverse-cube law the function $\alpha(d)$ is plotted as a solid line in Fig. 6. There are two scales for $\alpha(d)$ in this figure, shifted with respect to one another so that the comparison can be made with and without the dispersion and phase-shift corrections. Since these small corrections have been obtained completely independently of the calculation, the marked improvement in the agreement when they are added in provides an independent check on them. The first few points near 10 Å are probably off because the perturbation scheme implicit in the way the corrections are made is beginning to fail in thin films. (10 Å is about three statistical atomic layers of helium.) Probably the most exceptional and convincing feature of Fig. 6 is the way the experimental points and theoretical calculation both exhibit the same subtle deviation from the simple inverse-cube law due to retardation.

The calculations for CaF₂, SrF₂, and BaF₂ all give the same results for $\alpha(d)$ to within 2%. There is no simple reason why this should be the case, but the calculation does agree with the measurements. In order to demonstrate how insensitive the calculation is to the model parameters,

TABLE II. Dielectric parameters for CaF₂, SrF₂, and BaF₂.

Host	A_1	$\omega_1 \times 10^{-13}$ rad/sec	A_2	$\omega_2 \times 10^{-16}$ rad/sec (eV)	A_3	$\omega_3 \times 10^{-16}$ rad/sec (eV)	A_4	$\omega_4 \times 10^{-16}$ rad/sec (eV)	$n^2(0) - 1$ $= A_2 + A_3 + A_4$	N_{Eff} $= [\text{const}] \sum A_n \omega_n^2$
CaF ₂	4.33	5.03	0.772	2.13 (14)	0.102	3.57 (23.6)	0.162	5.25 (34.6)	1.036	11.9
SrF ₂	4.03	4.23	0.757	2.05 (13.5)	0.065	3.50 (23.1)	0.250	4.40 (29)	1.070	13.5
BaF ₂	4.40	3.56	0.727	1.83 (12.1)	0.069	2.74 (18.1)	0.359	3.65 (24.1)	1.155	14.5

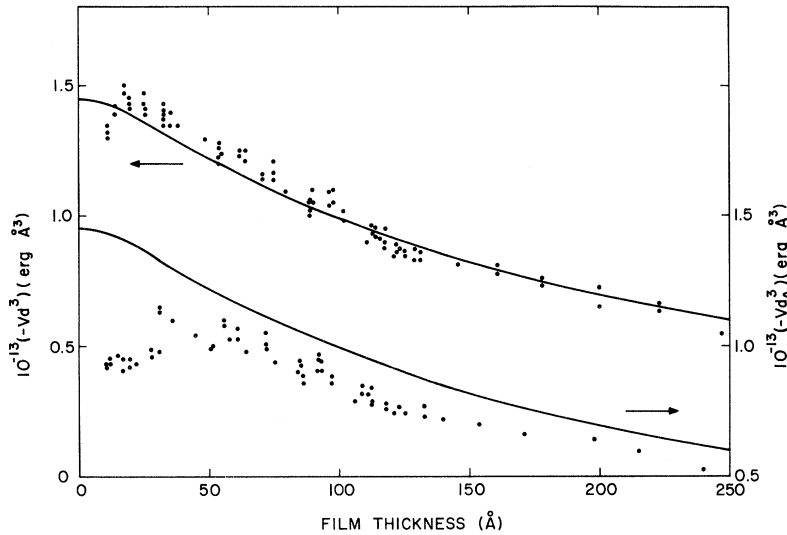


FIG. 6. van der Waals potential times the cube of the film thickness as a function of the film thickness. The solid lines are the theory of Lifshitz. The data points on lower half of graph are those for the uncorrected film thickness d_A , while the points on upper half of graph are those for which dispersion and phase-shift corrections have been added on.

the following series of calculations were carried out for the SrF_2 substrate. First of all, dropping the infrared band changes the potential at 250 Å, the point most sensitive to this band, by 1% and the film thickness by a negligible amount. When the center uv electronic band is dropped and the remaining two constants A_2 and A_4 adjusted to maintain the constraints on the optical index of refraction, the value of the potential changes less than 1% compared to the full-model calculation over the entire range 10–250 Å. The deviation in the calculated film thickness for a given value of the potential is given by curve 1 in Fig. 7. Variations in the position of the first band by ± 1 eV produced curves 2 and 3 in the same figure. Reducing the constant A_2 by one-half and increasing A_4 to maintain the correct optical index of refraction produce curve 4. If all the oscillator strength is put at the band at 13.5 eV so that it gives the correct index of refraction, then curve 5 is obtained. These last two extreme cases produce deviations in the calculated film thickness of at most ± 3 Å, which indicates that even very crude models of the dielectric function may be used to calculate the helium film thickness almost more accurately than even our very precise technique can measure it. However, the variation of the potential is sensitive to the model, especially in the very-small-thickness region, with curves 4 and 5 representing variations of $\pm 15\%$ in the potential at 10 Å. We conclude therefore that the agreement between the measurements and calculations given in Figs. 5 and 6 provides a real verification of the Lifshitz theory.

D. Calculations for Other Materials

Since the agreement between the theory and experiment is excellent for the alkaline-earth fluo-

ride crystals, the van der Waals potential has been calculated for a number of other materials using the full formula. The parameters used in the dielectric functions are given in Table III and the results for $\alpha(d)$ are plotted in Fig. 8. For some of the materials detailed information about the frequency dependence of the dielectric susceptibility is not known, but the film thickness is not very sensitive to the particular model used, as was demonstrated above. These plots should therefore be useful guides for calculating the film thickness on a variety of materials. Glass in particular should behave similarly to MgO , from which we must conclude that the thickness scale used by Rudnick *et al.*²⁷ for glass substrates must

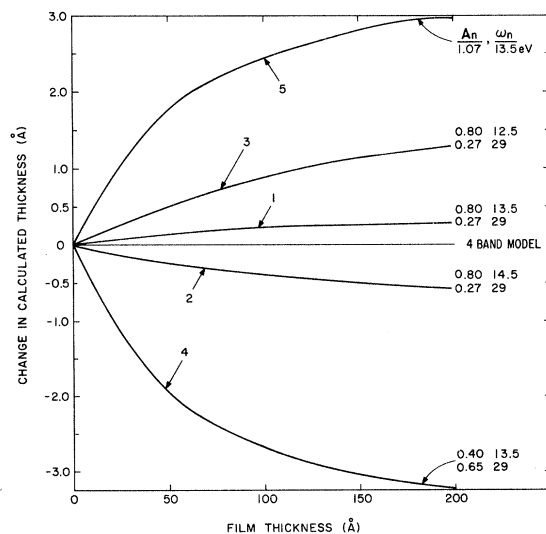


FIG. 7. Sensitivity in the calculated film thickness for a given potential value to different modes representing the dielectric function of the SrF_2 substrate.

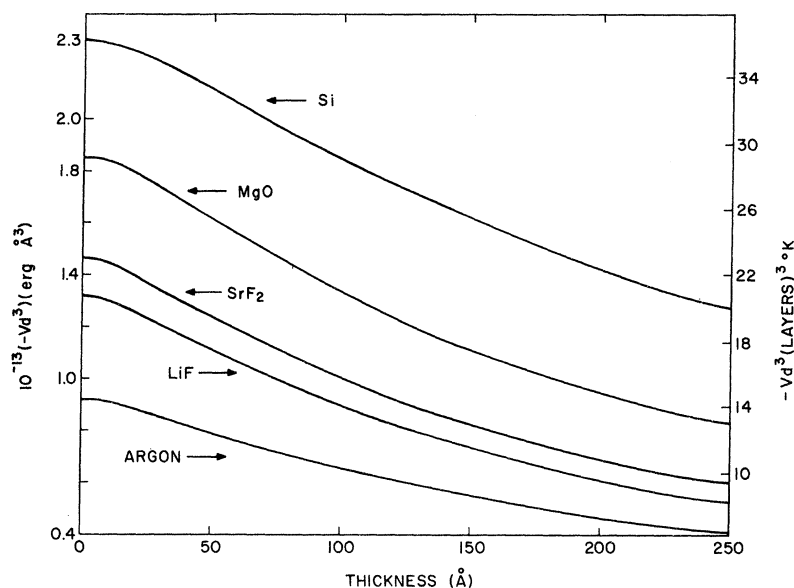


FIG. 8. Calculated curves of the van der Waals potential times the cube of the helium film thickness as a function of the film thickness for different dielectric substrates.

be almost 30–40% too large.

The calculations were also performed for metal substrates using a model dielectric response function given by

$$\epsilon_1(i\xi) = 1 + \omega_p^2 / \xi^2 \quad (17)$$

for plasma frequencies ω_p of 5, 10, and 20 eV. The results are shown in Fig. 9. Most metals have plasma frequencies near 5 eV, which exhibits a very good inverse-cubic law, since $\alpha(d)$ is almost constant over the range of thicknesses shown. This calculation gives film thicknesses of 240, 270, and 290 Å for a metal with an ω_p of 5, 10, and 20 eV, respectively, at a height of 1 cm.

E. Simplified Expressions for Theory

Because the dielectric susceptibility of liquid helium is very close to unity, the general expression given in Eq. (10) can be greatly simplified to

the following single integral:

$$V(d) = -\frac{\hbar}{8\pi^2 d^3} \int_0^\infty \left(\frac{\epsilon_1 - \epsilon_3}{\epsilon_1 + \epsilon_3} \right) \left(\frac{\epsilon_3 - 1}{\epsilon_3 + 1} \right) \times \left(1 + 2 \frac{\xi d}{C} \right) e^{-2(\xi d / C)} d\xi \quad (18)$$

This formula has the correct asymptotic behavior for both large and small d . A numerical calculation of this expression using the four-band model for SrF_2 deviates from the general expression by at most 8% for thicknesses between 10 and 250 Å.

It is often desirable to be readily able to obtain approximate values of the van der Waals potential in the two limiting regimes. A limiting expression for the thick-film region which is easy to use has been given by DLP.⁵ A simple expression for the thin-film region for helium films can also be readily derived. The integrand of Eq. (18) can be approximated in the following manner:

TABLE III. Dielectric parameters for LiF, MgO, Argon, and Silicon.

Crystal	A_1	$\omega_1 \times 10^{-16}$ rad/sec (eV)	A_2	$\omega_2 \times 10^{-16}$ rad/sec (eV)	A_3	$\omega_3 \times 10^{-16}$ rad/sec (eV)	A_4	$\omega_4 \times 10^{-16}$ rad/sec (eV)	$n^2(0) - 1$ $= A_1 + A_2 + A_3 + A_4$
LiF ^a	0.49	2.0 (13.2)	0.308	2.46 (16.2)	0.078	4.55 (30)	0.044	6.08 (40)	0.92
MgO ^b	1.539	1.58 (10.4)	0.417	2.88 (19)					1.95
Argon ^c	0.669	2.4 (15.8)							0.67
Silicon ^d	10.66	0.608 (4)							10.66

^aReferences 22 and 23.

^bReference 24.

^cReference 25.

^dReference 26.

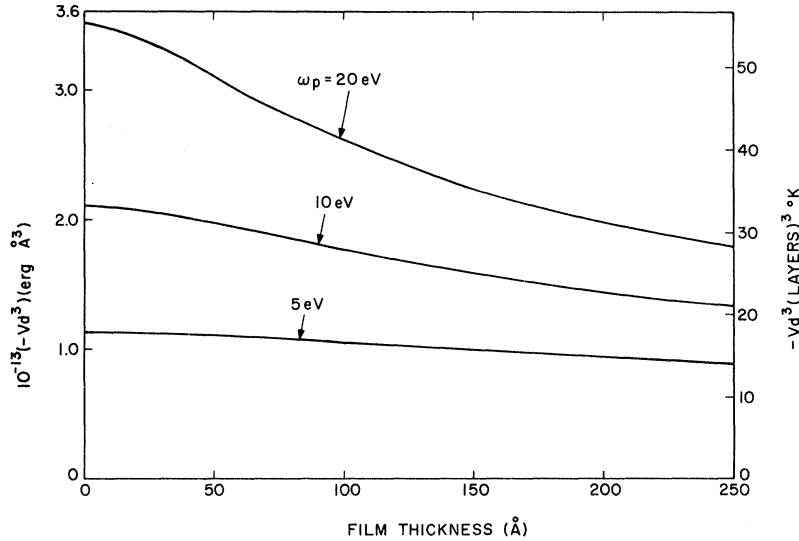


FIG. 9. Calculated curves of the van der Waals potential times the cube of the helium film thickness as a function of the film thickness for metals for three different dielectric functions.

$$\frac{\epsilon_1 - \epsilon_3}{\epsilon_1 + \epsilon_3} \frac{\epsilon_3 - 1}{\epsilon_3 + 1} \approx \left(\frac{\epsilon_1 - 1}{\epsilon_1 + 1} \right) \left(\frac{\epsilon_3 - 1}{\epsilon_3 + 1} \right) - \left(\frac{2}{\epsilon_1 + 1} \right) \left(\frac{\epsilon_3 - 1}{\epsilon_3 + 1} \right)^2. \quad (19)$$

The second term produces an integral which basically depends only on the properties of liquid helium. This second term for typical substrates like glass, SrF_2 , or metals in any case is less than 10% of the first term.

In the thin-film regime the van der Waals potential can be approximated by

$$V(d) = -\frac{\hbar\bar{\omega}}{8\pi^2 d^3 k} = -\frac{\alpha}{d^3}, \quad (20)$$

where

$$\bar{\omega} = \int_0^\infty \left(\frac{\epsilon_1 - 1}{\epsilon_1 + 1} \right) \left(\frac{\epsilon_3 - 1}{\epsilon_3 + 1} \right) d\xi.$$

$V(d)$ in Eq. (20) is given in $(\text{layers})^3 \text{ }^\circ\text{K}$. If desired, the second term in Eq. (19) could be included in the calculation. We now assume that the dielectric functions for both the helium and substrate can be characterized by single resonances with the entire oscillator strength as

$$\epsilon_3 = 1 + \frac{n_3^2 - 1}{1 + (\xi/\omega_3)^2}, \quad \epsilon_1 = 1 + \frac{n_1^2 - 1}{1 + (\xi/\omega_1)^2}, \quad (21)$$

where n_1 and n_3 are the optical indices of refraction and the ω 's are some suitable electronic frequency. Equation (20) can now easily be evaluated to give

$$\bar{\omega} = \frac{\pi}{2\sqrt{2}} \frac{(n_3^2 - 1)(n_1^2 - 1)}{[(n_3^2 + 1)(n_1^2 + 1)]^{1/2}}$$

$$\times \frac{\omega_1 \omega_3}{(n_3^2 + 1)^{1/2} \omega_3 + (n_1^2 + 1)^{1/2} \omega_1}. \quad (22)$$

This equation is similar to other approximations²⁸ which have been made to adapt the original London theory to condensed media, but we have not seen this particular form published elsewhere. The natural frequency to use for helium is 24.6 eV. For the other materials it is not a very bad approximation to use the frequency at which the pure substance becomes optically opaque at the edge of the intrinsic band-gap transition. This clearly gives a lower limit to $\bar{\omega}$, but, as the full calculation shows, the potential is less than that predicted by the simple inverse-cube law for thicknesses beyond 10 Å. The equation gives an α of 2.2 °K for the helium-helium case which should also in principle be subtracted from the above result. The results of this very simple calculation are given for a variety of materials in Table IV, and where possible a comparison to the full calculation is also given. The values of α from the approximate expression are within 10% of those obtained from the general expression. It is interesting to note that the original estimates given by Schiff¹⁰ in 1941 are quite reasonable.

We have developed a simple interpolation expression to give the film thickness on a SrF_2 substrate at 1.38 °K for a given van der Waals potential. It is

$$V(d) = \frac{A^3}{d^3 [1 + Bd(d+c)]^{1/2}}, \quad (23)$$

where $A = 5.30 \times 10^{-5}$, $B = 5.4088 \times 10^{-5}$, and $c = 1.316 \times 10^2$. This expression gives values for the film thickness which are within 0.2 Å of the general equation. One immediate application of

TABLE IV. Strength of the van der Waals potential for thin films ($d \rightarrow 0$) calculated using a simple one-band expression and the general formula.

Material	Simple one-band model				General expression	
	uv absorption $\omega \times 10^{-16}$ rad/sec (eV)	Optical dielectric constant n^2	$\alpha = -Vd^3$ (layers) ³ °K	$k = d H^{1/3}$ cm ^{4/3} $\times 10^8$	$\alpha = -Vd^3$ (layers) ³ °K	References
helium	3.73 (24.7)	1.057	2.2	130	...	19, 29
neon	3.26 (21.5)	1.2	6.7	187	...	19, a
argon	2.4 (15.8)	1.67	16.3	251	14.3	19, 25
krypton	2.12 (14)	1.80	18.3	261	...	19, 30
xenon	1.83 (12.1)	2.23	23.2	282	...	19, 30
NaF	1.64 (10.8)	1.74	14.6	242	15.7	21
LiF	2.0 (13.2)	1.92	19.7	268	20.6	22
KI	0.98 (6.5)	2.6	18.5	262	...	31
SrF ₂	2.05 (13.5)	2.07	22.4	280	22.8	21, 22
MgO	1.57 (10.4)	2.95	28.6	302	29.2	24
ORD.						
TiO ₂	0.61 (4)	5.91	26.2	294	...	32
Extra ord.						
Al ₂ O ₃	1.52 (10)	7.19	29.6	309	...	
silicon	0.61 (4)	3.25	31.4	312	...	22
metal	7.57 (5)	11.66	39	335	36.3	26
	1.52 (10)	...	20.5	271	17.8	
	2.28 (15)	...	36.3	328	33.2	
		...	49	362	...	

^aDielectric constant from Clausius-Mossotti equation.

knowing the thickness as a function of the potential is that it allows the resonance curves to be replotted as a function of film thickness, as shown in Fig. 10. The detailed shapes of these resonances are now open to investigation, which should provide insight into the attenuation of sound in liquid helium at these very high frequencies.

IV. COMPARISON OF FILM THICKNESS WITH PREVIOUS VALUES

There is a considerable amount of literature in this field and a complete review will not be attempted. However, it is rather clear that the reported values of the film thickness vary considerably and that the film thickness is an open problem.

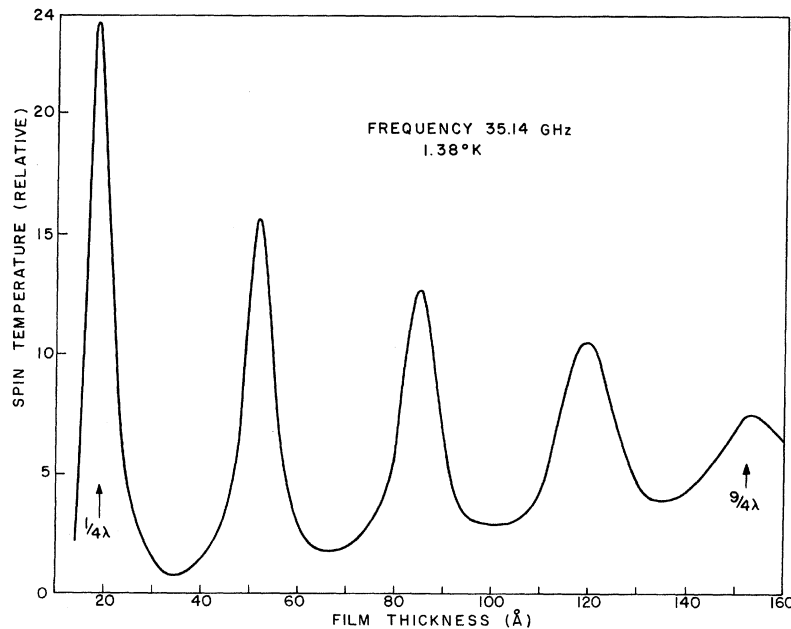


FIG. 10. Typical curve of the relative spin temperature as a function of the film thickness where the film thickness was calculated from the pressure readings using the equations in the text.

For the most part, the film thickness or the van der Waals coefficient was obtained predominantly by two methods. The adsorption-isotherm approach is used for unsaturated films and an optical-elliptometry technique for saturated films. The reported values of the thickness with some exceptions give some consistency as long as the comparison is made among values obtained by the same experimental technique. That is, the major disagreement on the film thickness occurs when comparing the results derived from different experimental techniques. Our present experimental results and calculations are in reasonable agreement with the film thicknesses obtained using the ellipsometric technique.

Using the ellipsometric technique, Jackson and co-workers³³ reported a thickness of about 310 Å at a height of 1 cm on a polished stainless-steel surface. Using the same technique, Hemming³⁴ reported a value of 323 Å for a height of 1 cm on gold-plated quartz. Our preliminary calculations given in this paper for the film thickness on metallic surfaces are consistent with these values. Hemming also obtained a value of 228 Å at a 1-cm height on quartz. This value is in good agreement with the calculated value presented in this paper, where we make the reasonable assumption that a MgO substrate would have a film thickness close to that of quartz. Our measured film thickness on a SrF₂ substrate using the technique described in this paper is 215 Å for a height of 1 cm.

In general, adsorption-isotherm measurements give thicker films for supposedly similar substrates. Bowers³⁵ using aluminum foil as a substrate reported a van der Waals constant $\alpha \approx 99$ (layers)³ °K or, equivalently, a film thickness of 460 Å at a height of 1 cm. A similar value of $\alpha = 87$ (layers)³ °K has been obtained²³ from an inverse-cube-law dependence over a restricted range of 1.7–2 helium layers adsorbed on argon-coated

sintered copper. There are a number of values reported for substrates of glass, with the most recent measurements³⁶ giving the lowest values of the van der Waals force. These latest values of α of 36 and 21 (layers)³ °K for porous glass and nitrogen-coated porous glass are more in line with the values reported by other measurement techniques. Our calculations for a glass substrate would predict a value of $\alpha = 29$ (layers)³ °K for thin films. Adsorption-isotherm measurements on graphite³⁷ give a value for $\alpha = 67$ (layers)³ °K. A recent experiment³⁸ using a new technique, in which the change in the resonant frequency of a quartz crystal owing to the mass loading of the helium film is measured, reported a value for $\alpha = 39$ (layers)³ °K.

V. CONCLUSIONS

The exceptionally good agreement between the film-thickness measurements and those calculated using the Lifshitz formula leaves very little uncertainty about the thickness of liquid-helium films on atomically flat regions of the alkaline-earth fluorides. Previous measurements^{33,34} using the elliptometry technique are also in rather good agreement with the theory. With the exception of the work of Evenson *et al.*,³⁶ the adsorption-isotherm measurements on unsaturated films gave much stronger van der Waals forces and correspondingly thicker films. A possible explanation of the stronger forces is that most isotherm measurements were restricted to films only a few atoms thick and the results cannot be extrapolated into the thicker-film region with any confidence. The surface roughness in these experiments is certainly significant. Thus it is our conclusion that the film thickness, when greater than the surface roughness, can be obtained from the Lifshitz formula with great precision.

¹D. van der Waals, *Die Kontinuität des Gasformigen und Flüssigen Zustandes* (Amsterdam, 1881).

²F. London, *Z. Physik* **63**, 245 (1930).

³H. B. G. Casimir and D. Polder, *Phys. Rev.* **73**, 360 (1948).

⁴E. M. Lifshitz, *Zh. Eksperim. i Teor. Fiz.* **29**, 94 (1955) [*Sov. Physics JETP* **2**, 73 (1956)].

⁵I. E. Dzyaloshinskii, E. M. Lifshitz, and L. P. Pitaevskii, *Advan. Phys.* **10**, 165 (1961).

⁶V. A. Parsegian and B. W. Ninham, *J. Chem. Phys.* **52**, 4578 (1970); *Biophys. J.* **10**, 646 (1970); *Biophys. J.* **10**, 664 (1970).

⁷V. B. Derjaguin and I. I. Abrikosova, *Discussions Faraday Soc.* **18**, 33 (1954).

⁸J. A. Kitchener and A. P. Prosser, *Proc. Roy. Soc. (London)* **A242**, 403 (1957); W. Black, J. G. V. de Jongh, J. Th. G. Overbeek, and M. J. Sparnaay, *Trans. Faraday Soc.* **56**, 1597 (1969); A. Van Silfhout, *Proc. K.*

nede. Adad. Wet **69B**, 501 (1966).

⁹D. Tabor and R. H. S. Winterton, *Proc. Roy. Soc. (London)* **A312**, 435 (1969); J. N. Israelachvili and D. Tabor, *Nature* **236**, 106 (1972).

¹⁰L. Schiff, *Phys. Rev.* **59**, 839 (1941).

¹¹P. Richmond and B. W. Ninham, *J. Low Temp. Phys.* **5**, 177 (1971); *Solid State Commun.* **9**, 1045 (1971).

¹²C. H. Anderson and E. S. Sabisky, *Phys. Rev. Letters* **24**, 1049 (1970).

¹³C. H. Anderson and E. S. Sabisky, in *Physical Acoustics*, edited by W. P. Mason and R. N. Thurston, (Academic, New York, 1971), Vol. 8, Chap. 1.

¹⁴It is possible to detect the spin temperature using the reflected microwave power with the crystal mounted in a standard microwave cavity, which would allow the film thickness to be measured on a wider range of materials. The tuning range of the microwave frequency is limited, however, and care has to be taken not to produce heating

effects through eddy currents if the standard field-modulation technique is used.

¹⁵W. H. Strehlow and E. L. Cook, *Phys. Rev.* **188**, 1256 (1969); N. Bezerianos and R. W. Vook, *J. Appl. Phys.* **43**, 1417 (1972).

¹⁶C. H. Anderson and E. S. Sabisky, *Phys. Rev. Letters* **28**, 80 (1972).

¹⁷B. L. Blackford, *Phys. Rev. Letters* **28**, 414 (1972).

¹⁸V. A. Parsegian and B. W. Ninham (private communication).

¹⁹G. A. Cook, *Argon, Helium and the Rare Gases* (Interscience, New York, 1961), pp. 141-148; W. H. Kesom, *Helium* (Elsevier, London 1942), p. 422.

²⁰D. R. Bosomworth, *Phys. Rev.* **157**, 709 (1967).

²¹G. W. Rubloff, *Phys. Rev. A* **5**, 662 (1972).

²²G. Stephan, Y. LeCalvez, J. C. Lemonier, and S. Robin, *J. Phys. Chem. Solids* **30**, 601 (1969); G. Stephen, J.-C. Lemonier, and S. Robin, *J. Opt. Soc. Am.* **57**, 486 (1967); T. Tomiki and T. Miyatu, *J. Phys. Soc. (Japan)* **27**, 658 (1969).

²³*American Institute of Physics Handbook* (McGraw-Hill, New York, 1963), Chap. 6.

²⁴D. M. Roessler and W. C. Walker, *Phys. Rev.* **159**, 733 (1967).

²⁵A. J. Eatwell and G. O. Jones, *Phil. Mag.* **10**, 1059 (1964).

²⁶G. Dresselhaus and M. S. Dresselhaus, *Phys. Rev.* **160**, 649 (1967).

²⁷I. Rudnick, R. S. Kagiwada, J. C. Frasier, and E. Guyon [*Phys. Rev. Letters* **20**, 430 (1968)] give a formula for the thickness which they obtained from W. M. McCormick *et al.* [*Phys. Rev.* **168**, 249 (1968)]. This formula has since been used by several authors as a general guide for the thickness.

²⁸H. Buttner and E. Gerlach, *Chem. Phys. Letters* **5**, 91 (1970); H. Krupp, *Advan. Coll. Interface Sci.* **1**, 111 (1967).

²⁹C. J. Grebenkemper and John P. Hagen, *Phys. Rev.* **80**, 89 (1959).

³⁰Giancarlo Baldini, *Phys. Rev.* **128**, 1562 (1962).

³¹H. R. Philip and H. Ehrenreich, *Phys. Rev.* **131**, 2016 (1963).

³²Manual Cardona and Gunther Harbeke, *Phys. Rev.* **137**, A1467 (1965).

³³L. G. Grimes and L. C. Jackson, *Phil. Mag.* **4**, 1346 (1959); A. C. Ham and L. C. Jackson, *Proc. Roy. Soc. (London)* **A240**, 243 (1957).

³⁴D. Hemming, *Can. J. Phys.* **49**, 2621 (1971).

³⁵R. Bowers, *Phil. Mag.* **44**, 485 (1953).

³⁶A. Evenson, D. F. Brewer, A. J. Symonds, and A. L. Thomson, *Phys. Letters* **33**, 35 (1970).

³⁷J. A. Herb and J. G. Dash, *Phys. Rev. Letters* **29**, 846 (1972).

³⁸M. Chester, L. C. Yang, and J. B. Stephens, *Phys. Rev. Letters* **29**, 211 (1972).